

Late Sveconorwegian monzonitic dykes in the Setesdalen area of Central South Norway: Examples of structures in dykes and their indications of accumulated strain

LILIAN SKJERNAA & SVEND PEDERSEN



Skjernaa, L. & Pedersen, S. 2000–02–10. Late Sveconorwegian monzonitic dykes in the Setesdalen area of Central South Norway: Examples of structures in dykes and their indications of accumulated strain. *Bulletin of the Geological Society of Denmark*. Vol. 46, pp. 203–223. Copenhagen.

In the Setesdalen area, Central South Norway, a large number of monzonitic dykes and other minor bodies were intruded during the late stages of emplacement of Sveconorwegian magmatic complexes. Some of the dykes define cone sheet and bell-jar sheet systems. The dykes possess internal linear and planar fabrics, which are not seen in any of the host rocks. Also, cross-cutting granitic veins within the dykes are deformed and may show ptygmatic folds, whereas in the host rocks these same veins appear undeformed. The internal strain in the dykes was determined from vein deformation to be mainly simple shear with or without a volume reduction. The strain preferentially accumulated in the ductile monzonite dykes while the more rigid host rock blocks were passively displaced. In some cases, an additional minor component of flattening affected both the dykes and their host rocks.

Key words: Foliated dykes, monzonite dykes, strain analysis, ptygmatic folds, cone sheets, bell-jar sheets, ring intrusion, central intrusion, Setesdalen, Sveconorwegian.

L. Skjernaa [lilians@geo.geol.ku.dk] & S. Pedersen [svendp@geo.geol.ku.dk]
Geological Institute, University of Copenhagen, Øster Voldgade 10, DK-1350
Copenhagen K, Denmark. 8 March 1999.

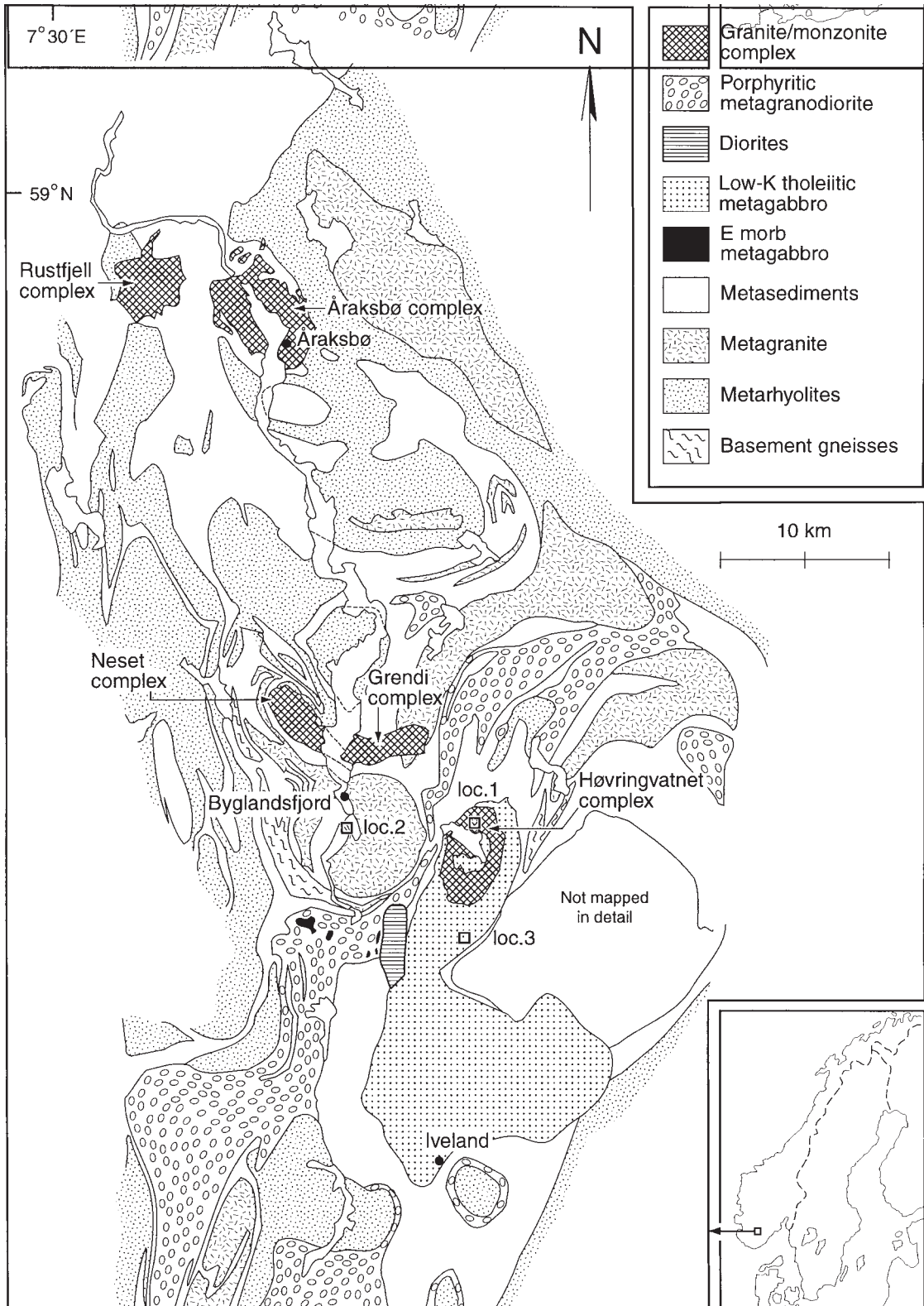
One of the most conspicuous geological features in the Setesdalen area of Central South Norway is a large number of small, light-grey, often spotted, more or less irregular monzonitic dykes and bodies, which belong to the Setesdalen Igneous Province (Pedersen & Konnerup-Madsen 2000). They cross-cut all major rock types in the area except some pegmatites, and are emplaced during the waning stage of the Sveconorwegian Orogeny. Many of the small intrusions are bimodal, with both a monzonitic and a granitic component, and often have cusped boundaries. In spite of their late intrusion, they generally possess a pronounced internal fabric, not found in their host rocks.

Highly deformed dykes occurring in undeformed or less-deformed country rocks have been described from many places in the world in a variety of geological settings and dyke compositions (Miller 1945, Kaitaro 1953, Johnson & Dalziel 1966, Allart 1967, Watterson 1968, Berger 1971, Davidson & Park 1978). The disparity in fabric between the dyke and host rocks was attributed to a molten or at least hot state of the

dyke rocks and their selective straining through localized shearing between rigid country rock blocks during or immediately after consolidation of the dykes. Cusped boundaries have also been interpreted as primary features that reflect syn-emplacement deformation or -movement.

Talbot (1982) and Talbot & Sokoutis (1992) on the other hand strongly advocated a simultaneous and equal deformation of the dykes and country rocks, during which the dykes rotated as incompetent layers. The cusped character of some contacts were thought to be mullion structures and thus to have formed rather during a later regional deformation. They ascribed the lack of fabric development in the host rocks not to a lack of strain, but to the country rock fabric being less responsive to strain.

Ryan (1995) investigated whether the internal fabric in the dykes, the cusped margins and the irregular forms of the dykes are primary syn-intrusion features or are formed later as superimposed deformational phenomena. From foliated dykes in the Nain area,



Labrador he found mineralogical and metamorphic evidence for both scenarios.

In the Setesdalen area, both the monzonite dykes and their host rocks are in many places penetrated by granitic and pegmatitic veins which are distorted, folded or stretched inside the monzonites, but appear undeformed in the host rock. An analysis of the deformational structures of these veins may contribute new aspects to the discussion.

This paper describes the occurrence and intrusive character of these minor monzonitic bodies and dykes, their internal fabric and deformation structures and presents the results of strain analyses that were carried out at three localities.

Regional setting

The Precambrian basement of southern Norway is divided by a number of low angle thrusts into crustal segments with various crust-forming histories (Berthelsen 1980, 1987). The westernmost segment, where the Setesdalen area is situated, is dominated by structures formed during the Sveconorwegian Orogeny (Pedersen & Konnerup-Madsen 2000). The Sveconorwegian Orogeny is usually considered to be delimited by ages of 1250 and 900 Ma (Falkum & Pedersen 1980, Skjerna & Pedersen 1982, Park et al. 1991, Starmer 1993, Andersen et al. 1994, Bingen et al. 1996). However, in the Setesdalen area, it appears that the main Sveconorwegian event is younger than 1100 Ma with the main deformations occurring about 1000 Ma (Falkum & Pedersen 1979, Pedersen & Konnerup-Madsen 2000).

During the waning stages of the Sveconorwegian Orogeny, chemically evolved igneous rocks intruded into the central part of the southern Norway around the Setesdalen Valley. These rocks constitute the Setesdalen Igneous Province and they include an older group consisting of a bimodal diorite-granodiorite complex with accompanying Ni-mineralisations and a younger group of five, bimodal complexes with granitic and monzonitic compositions (Fig. 1). A fundamental aspect of the Setesdalen Igneous Province is its chemical character: potassic to ultrapotassic alcalic composition and high concentrations of Sr, Ti, Zr, P, Ba and LREE. The overall geology and regional setting of the Setesdalen area are described by Pedersen & Konnerup-Madsen (2000), see also Pedersen (1975, 1981) and Hansen et al. (1996).

The youngest intrusive complexes

In the southern Setesdalen valley, some of the youngest magmatic complexes exhibit magmatic layering of cm to m scales as well as subvolcanic structures such as cone sheets, radial dykes and bell jar intrusions. Associated with these complexes are presumably some of the abundant occurrences of pegmatites, famous for their rare minerals (Bjørlykke 1934, 1937).

The plutons all contain a granitic and a monzonitic component, varying in proportions. In general, the relations between the two components are complex with highly irregular boundaries and contradicting age relationships, leading to the impression that they represent largely immiscible melts that were intruded contemporaneously into a heated crust. Usually the two components are clearly separated, with the monzonite lying below the granite, but often a zone of hybrids have formed between the two.

A huge number of small, fine-grained monzonite and/or granite-aplite intrusions are either emplaced into the larger plutons, or are found in their vicinity, indicating a close genetic relationship between them. In addition to the minor bodies and dykes, which are spatially associated with the five intrusive complexes, numerous similar minor intrusives of meter or decimetre size are scattered from Iveland in the South to Åraksbø in the North (Fig. 1). A few occurrences have even been observed further north to north of Valle (about 12 km north of the map in Figure 1), suggesting that additional intrusive complexes may be present to the north and at depth.

The Høvringsvatn Complex. Of the five complexes, the Høvringsvatn Complex (Fig. 2) has been studied in most detail. It is emplaced into metagabbroic rocks (amphibolite in Figure 2). The Høvringsvatn Complex is a typical ring- or central complex (Pedersen & Konnerup-Madsen 2000) and exhibits the typical features that are related to subterranean cauldron subsidence, see Anderson (1936) and Roberts (1970).

The present topographic level cuts the top of the intrusion very close to the roof, exposing a pattern of xenoliths and roof-pendants which follow the ring pattern developed in the complex. The two main rocks in the pluton are a dark medium-grained and a lighter grey medium-grained isotropic monzonite, overlain by a medium- to coarse-grained granite. In the south-eastern part of the intrusion, the granite is finer grained. The ring pattern is clearly outlined by the occurrences of several cone sheet systems which cross-cut all major rock types in the area except the pegmatites. Each system includes a large number of cone sheets, most of which are too narrow to be shown on Figure 2, in some places up to about 20 closely-spaced sheets are visible. The inner and outer cone systems mainly consist of monzonite sheets, while the system in between includes granitic sheets. Some cone sheets suggest multiple intrusion because they contain two or three

←
Fig. 1. Geological map of the Setesdalen area. Loc. 1-3 are localities where detailed structural investigations has been carried out.

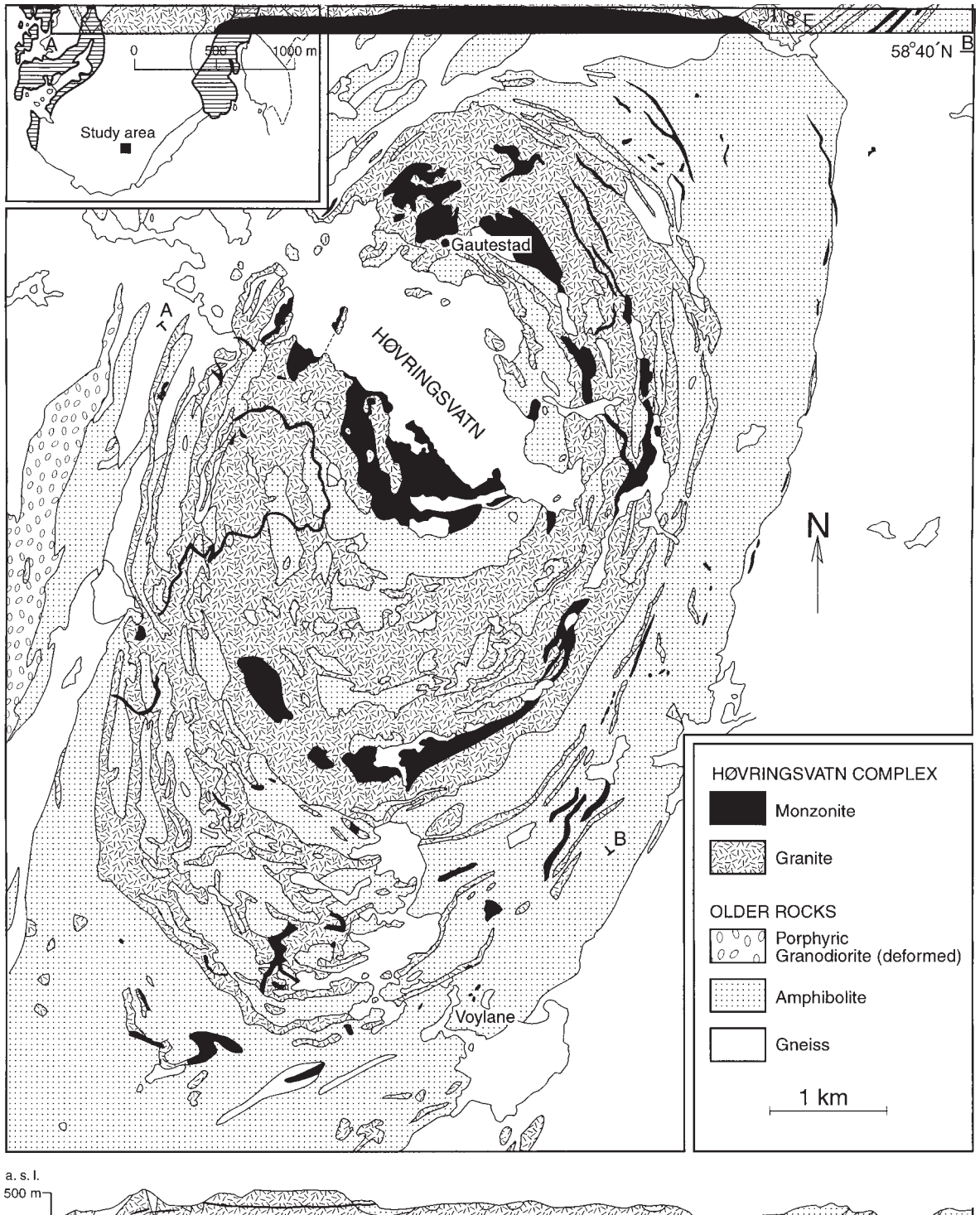
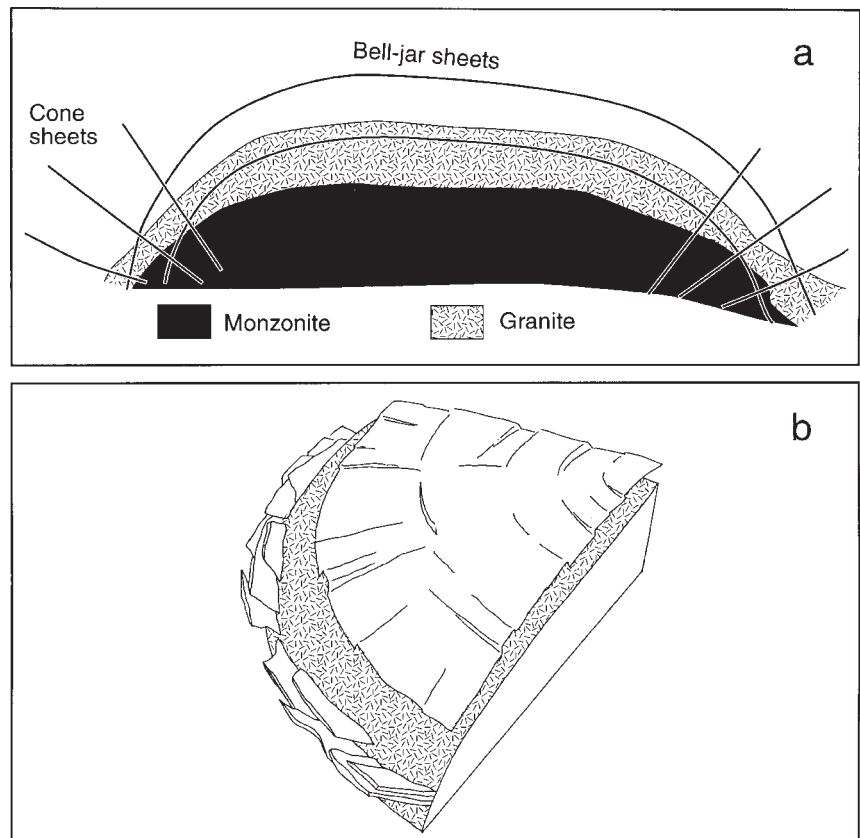


Fig. 2. Geological map and cross section of the Høvringsvatn area, for simplicity the pegmatites in the area are omitted.

Fig. 3. Simplified profile (a) and block diagram (b) outlining the cone sheets and bell-jar sheets in the Høvringsvatn area.



phases of monzonite. Many monzonitic sheets have marginal veins of aplitic granite and also contain many narrow aplitic sheet veins. Subhorizontal fine-grained monzonite intrusions of a bell-jar type cut all types of rocks. Both the cone and the bell-jar sheets often have irregular outlines and boundaries (Fig. 3). The cone sheets often have a limited extend in the outcrop and form a complex three dimensional network. Radial dykes are observed at a few localities along the shore of Lake Høvringsvatn. Associated with the Høvringsvatn Complex are several generations of minor dykes and irregular bodies which do not clearly fit into the cone or bell-jar dyke systems, but which occur as scattered bodies in the topographically lower part of the complex, especially on the bottom of Lake Høvringsvatn.

The cross-cutting relationships of the minor monzonite and associated granite aplitic intrusions clearly place these as being some of the youngest rocks in the Setesdalen area. Rb-Sr age determinations of the granite in the Høvringsvatn pluton yielded 945 ± 53 Ma with an initial Sr isotope ratio of 0.7041 ± 0.0007 , while an age of 900 ± 53 Ma and an initial Sr isotope ratio of 0.7040 ± 0.0002 were obtained from the monzonitic cone sheets (Pedersen 1981).

The minor monzonite intrusions

Shapes and contact relationships

The monzonite dykes and minor intrusive bodies in the Setesdalen area are structurally and chronologically remarkable, because they bear witnesses to an internal deformation that does not appear to have affected their host rocks, regardless of whether the host rock belongs to one of the intrusive complexes or is an older gneiss or amphibolite. Where the dykes have been intruded into a gneissic or banded host rock, they cut the host rock fabric discordantly without any signs of marginal deformation (Figs 4a, 4b).

Although, many of the minor monzonite intrusions outline systems of cone and bell-jar sheets, they may show bifurcating, branching and anastomosing patterns (Fig. 2). At the local scale, they appear as separate elongate bodies of strongly deformed monzonite enclosed in undeformed country rock. Undeformed, as used here, means that the host rock was not affected by the deformation that formed the internal fabric and structure in the monzonite. Where the host rock is an isotropic granite or monzonite, the minor monzonite bodies are easily misinterpreted as xenoliths and thus to have a reverse age relationship to the host rock. Such relationships were also observed by Miller (1945).

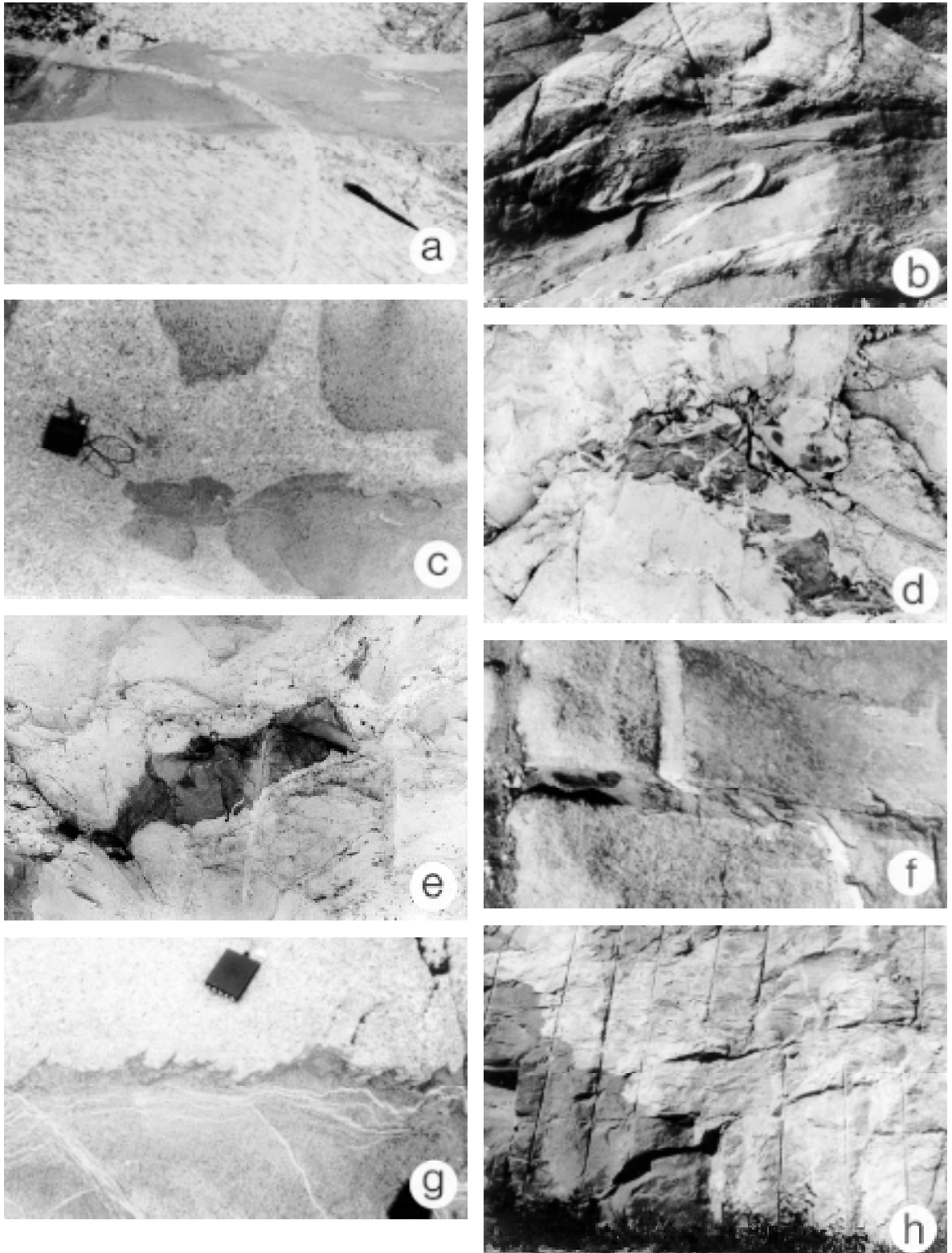


Fig. 4. Examples of shapes, margins and internal structures of monzonite dykes and other minor monzonite bodies (dark on the photographs). b is from loc. 3, h from loc. 2. See text for further explanations. Approximate heights of photos: a: 75 cm, b: 1.5 m, c: 60 cm, d: 75 cm, e: 60 cm, f: 75 cm, g: 50 cm, h: 4 m.

Some minor monzonite bodies occur as enclaves in the granite or in the isotropic, medium-grained monzonite. They may have rounded globular shapes, and sometimes have lobate margins (Fig. 4c) or are flattened and attenuated. Wiebe & Collins (1998) regarded such enclaves as being intruded as swarms through the granitic cumulate at the base of the magma chamber, into the still molten, crystal-poor magma where they spread over the top of the cumulate. Their flattened shapes and internal fabric are thought to have formed during the enclave emplacement and their deposition and compaction in the magma chamber. Another type of minor monzonite bodies, which are also observed in a gneissic host rock, have amoeboid shapes (Fig. 4d), while others are subangular (Fig. 4e).

Some monzonite dykes have plane parallel walls (Figs 4a, 4f) that may contain offsets at angular steps, but many of the dykes are irregularly shaped and have lobate/cusped irregularities at their contacts (Figs 4g, 4h). The cusps are formed by the dyke rocks and the lobes by the host rocks, indicating that during the formation of the cusps, the dyke rock was less competent than the host rock (Ryan 1995). Some cusps are very long and narrow, taking the form of apophyses. The tendency to form irregular contact relationships is most prominent when the host rock is acidic as is the case with the granite belonging to the Høvringsvatn Complex and the acid gneisses found to the west of the complex. In a few cases, melting of granitic gneiss host with accompanying back veining is observed. The hosts that have produced melts have nearly cotectic compositions at rather low pressures of about 5 Kb (Pedersen 1981) indicating that the level of emplacement is intermediate to high. The dykes that intruded into more basic host rocks such as the amphibolite around the Høvringsvatn Complex, have straighter boundaries, but even these show some curved contacts. The terminations of the dykes are flamed, tentaculate, or simply thin out to form a lanceolate termination. Some fracturing or a faint foliation in the host rock is sometimes observed in the lateral continuation of the dyke.

Characteristic for many, but far from all, of the monzonite dykes is that in addition to the monzonitic phase, they also contain a granitic phase, which seems to have been emplaced at the same time. The granitic phase mostly occurs as contact aplites (Fig. 4a) and as thin sheet veins (Figs 4g, 5a) which may be folded (Figs 5b, 5c) in the monzonite dykes. Xenoliths are present in the granitic part while they are rare in the monzonitic part.

Fabric in the monzonite dykes

Internally, the monzonite dykes possess a more or less well-defined fabric which may be linear, planar, or a combination. The fabric is outlined by the parallel ar-

rangement of dark minerals (biotite and/or amphibole) or by flattened aggregates of dark minerals (Figs 6a, 6b). The orientation of the fabric is sometimes oblique to the contacts of the dyke, but is often subparallel with it, especially in narrow dykes. Sigmoidal oblique fabrics across the dykes are seen, but mostly the bulk strain appears quite homogenous across the dyke.

Crosscutting granitic veins

Most of the dykes are crossed by granitic veins of aplitic to pegmatitic grain size. The veins are mostly a couple of millimetres to a couple of centimetres thick, but pegmatites up to some tens of centimetres are found. The orientational distribution of the veins ranges from parallel to perpendicular to the dyke margins. Some of the veins cross the margins of the dykes and can be traced for shorter or longer distances in the host rock (Figs 4a, 4b, 4f, 5a, 5d, 5e). Where veins cross the boundary between the host rock and the dyke, they usually take up a new orientation, but no examples of disruption and displacement of the vein have been observed at the dyke contacts. Some veins, however, terminate at or close to the boundary of the dyke. Within the dykes, the veins show beautifully developed deformation structures in the form of folds, mostly pygmatic (Figs 5d, 5e, 5f), pinching and boudinage (Figs 4b, 4f), clearly indicating that some veins have been shortened and others stretched. (For definition of pygmatic folds and a discussion of their origin, see Kuenen (1967)). It is immediately striking that although these structures are indicative of a rather strong deformation inside the monzonite, the host rocks outside the monzonites appear unaffected by this deformation, and the veins in the host rocks show no deformation structures.

In those monzonites which contain deformed felsic veins, the fabric has probably formed, or has at least been transposed, during post-emplacement deformation. Generally, the orientation of the fabric agrees with the sense of lateral displacement across the dyke which is inferred from the lateral displacement and reorientation of cross-cutting veins (Figs 4a, 4b, 4f, 5e). In detail, the foliation often reflects the folds in the pygmatic veins showing divergent fans close to the fold hinges (Fig. 5g).

The felsic veins have been emplaced into a set of multiply oriented, largely planar joints, during a period of dilatation and prevailing brittle conditions. This period clearly postdated the more ductile conditions that prevailed during the intrusion of the dykes and marks a chronological separation between the intrusion of the dykes and the development of their internal structures. During their deformation, the veins were more competent than the monzonitic dyke rock, which on the other hand was less competent than the host rocks.

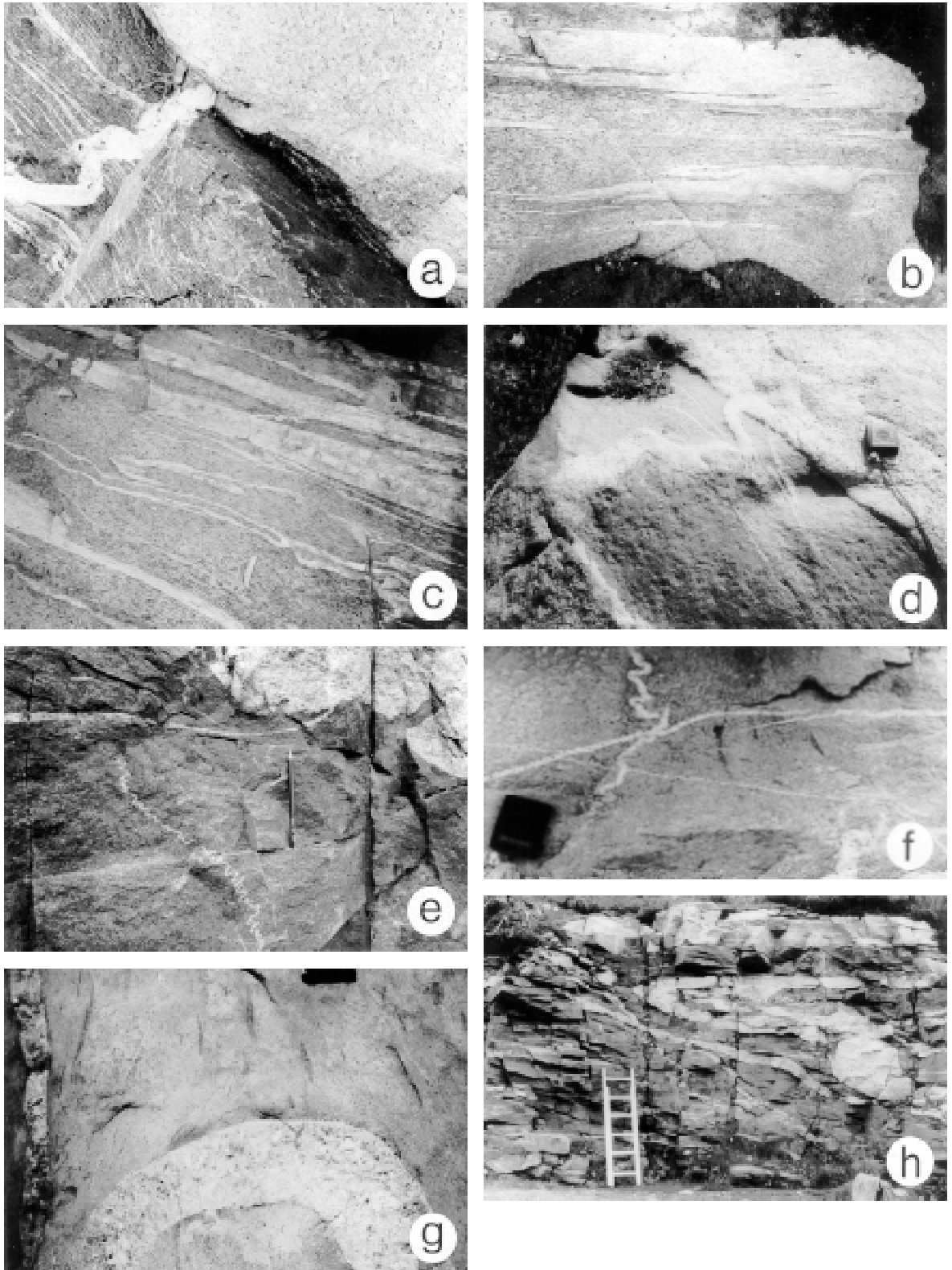


Fig. 5. Examples of shapes, margins and internal structures of monzonite dykes and other minor monzonite bodies (dark on the photographs). a, b and c are from loc. 3, e and f are from loc. 2, h show part of the outcrop at loc. 1 with structures cut at a low angle to the foldaxes. See text for further explanations. Approximate heights of photos: a: 75 cm, b: 60 cm, c: 60 cm, d: 80 cm, e: 50 cm, f: 40 cm, g: 35 cm, h: 4.5 m.

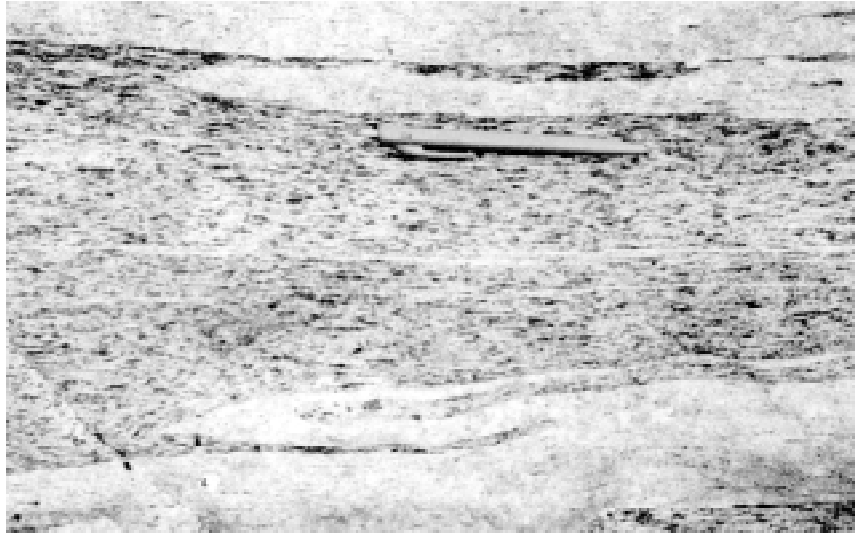
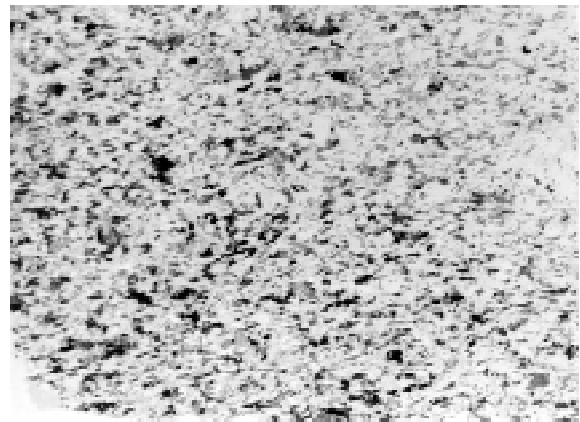


Fig. 6. Above: strongly foliated and lineated monzonite dyke with folded granitic sheets, the lineation is almost parallel to the surface of the outcrop, locality 3, ball pen as scale. Right: thin section showing foliation in a monzonite dyke (plane light), the monzonite also contains a lineation which is perpendicular to the section. Horizontal length of photo is 2 cm.



Locality descriptions

Detailed studies of monzonite dykes and their internal structures have been carried out at three localities (Fig. 1) where the monzonite dykes contain a large number of veins some of which cross the boundary to the host rock. Below the three localities are described and an attempt is made to quantify the internal strains in the dykes.

Locality 1

The first site is a road cut north-east of the farm houses in Gautestad. A flat lying monzonite, which forms part of a bell jar structure in the Høvringsvatn Complex, cuts through the granite of this complex. The granite in this part of the pluton is porphyritic with a weak foliation that probably developed prior to the dyke intrusion. The dyke wedges out at one end and a local, rather distinct foliation in the granite seems to have developed by shearing in its lateral continuation.

At a neighbouring locality, the bell jar sheet cuts a monzonitic cone sheet. The bell jar sheet has a foliation dipping at a low angle south and a lineation defined by elongate aggregates of dark minerals plunging down dip. The dyke contains many aplitic and granitic veins frequently folded inside the dyke, suggesting a shortening of the steeply inclined veins (Fig. 5h).

Locality 2

This site on both sides of the main road (Fig. 7) near the dam south of the village of Byglandsfjord (Fig. 1) demonstrates the contact relationships and structures of cross cutting veins (Figs 4h, 5e, 5f). The host rock is a migmatitic, light reddish-grey granitic orthogneiss and the dyke rock is fine-grained with only small patches of dark mineral aggregates. The dyke may have formed in connection with the Høvringsvatn Complex, but it is more likely related to the Grendi Complex

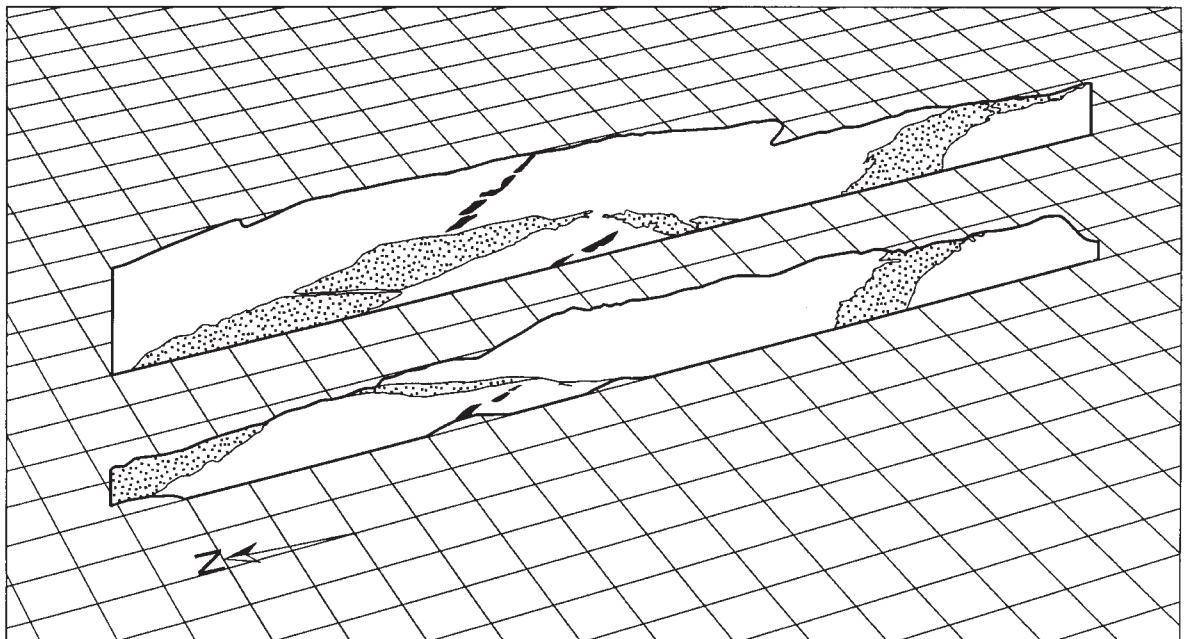
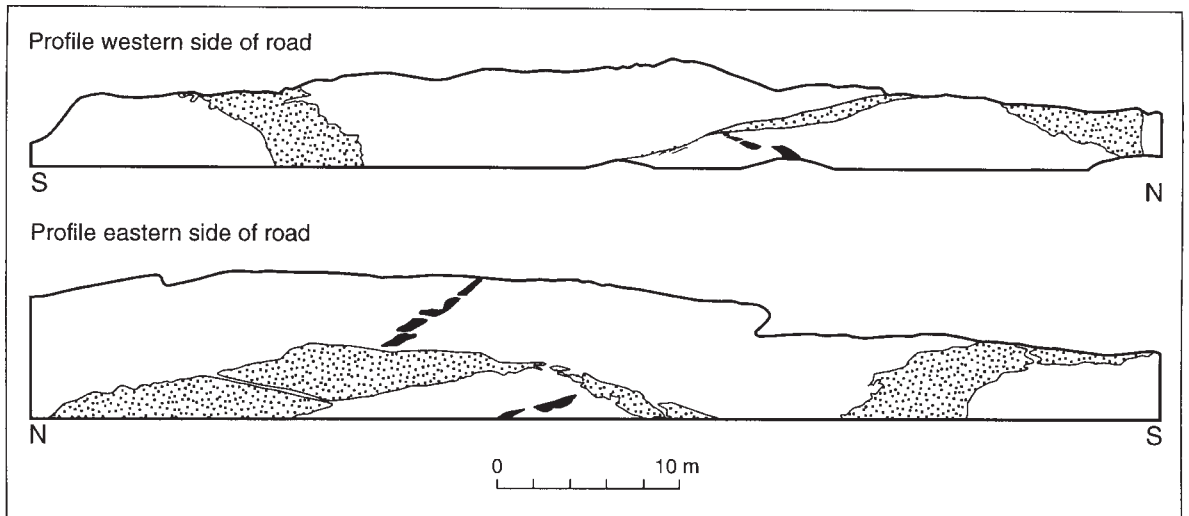


Fig. 7. Above: Road cuts at locality 2, no vertical exaggeration. Below: set piece diagram showing relative position of the road cuts. Side length of squares is 2m.

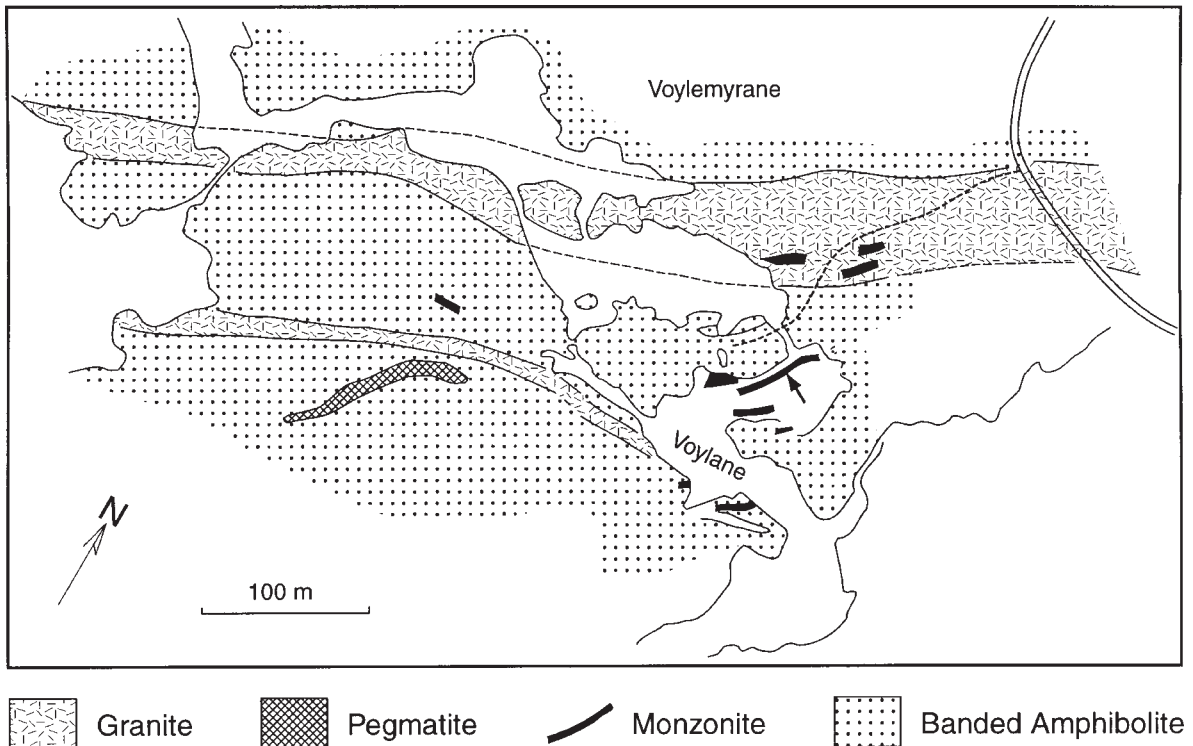


Fig. 8. Geological map of the area around Voylane (loc. 3). Stippled heavy line is a foot path from the gravel road in the upper right corner towards the locality. Arrow points to the monzonite dyke that was subjected to detailed structural investigations. The dyke is only visible at low water levels in Voylane.

(Fig. 1). The shape of the dyke and the displacement of an older, boudinaged, ultramafic amphibolite dyke (Fig. 7) indicates, that the mechanism of intrusion was that of transtension (Baer & Blyth 1990). In the exposed sections, the dyke has the form of two rhombic bodies connected by a narrow, parallel sided or wedge shaped part (Fig. 7). Parts of the contacts show irregular and cusped structures (Figs 4h, 7). The internal fabric is difficult to measure accurately because of the fine-grained character of the dyke.

A large number of granitic veins transsect the dyke and some of them continue with a different direction into the gneiss (Fig. 5e). Where they cross-cut the gneiss they follow an angular course, but show no visible signs of deformation. Inside the dyke, many of them are pygmatically folded into class 1B folds with wavelengths proportional with the thickness of the veins characteristic of buckled single layers in an incompetent matrix (Ramberg 1960, Kuenen 1967, Ramsay 1967, Skjerna 1975, Ramsay & Huber 1987).

While steep veins are folded, flat-lying veins are mostly planar (Figs 5e, 5f) but some show boudinage or pinching. One vein has both folds and boudins and may thus bear witness to a progressive structural evolution. The scarcity of veins with both folds and boudins indicates that shortening of veins is generally fully reversible (Talbot 1970).

Locality 3

Around the small lakes at Voylane, there are several exposures in the outer cone sheet system within the south-eastern part of the Høvringsvatn Complex (Fig. 8). At the locality strongly sheared monzonites with folded internal sheet veins as well as folded or boudinaged cross-cutting aplite and pegmatite veins are exposed.

The dykes constitute a swarm of cone sheets, each of which generally does not exceed a few meters in width. Contacts to the amphibolitic host rock (a banded metagabbro) are sharp and relatively planar, and the banding in the amphibolite is cut at a large angle by the dykes (Fig. 4b). Along the strike the sheets fade out, and usually they have a maximum length of about 100 meters. A few xenoliths of metagabbro are occasionally found in the dykes.

The monzonites have a strong internal fabric defined by abundant parallel biotite aggregates that are up to 1 cm long (Figs 5b, 5c, 6a).

Within the monzonite dykes, light grey, fine-grained granitic veins or thin sheets occur, which may have formed from a felsic component in the bimodal magma that invaded the dykes. These veins are often isoclinally folded with nearly horizontal axes subparallel to the contacts of the dykes (Figs 5b, 5c). Younger

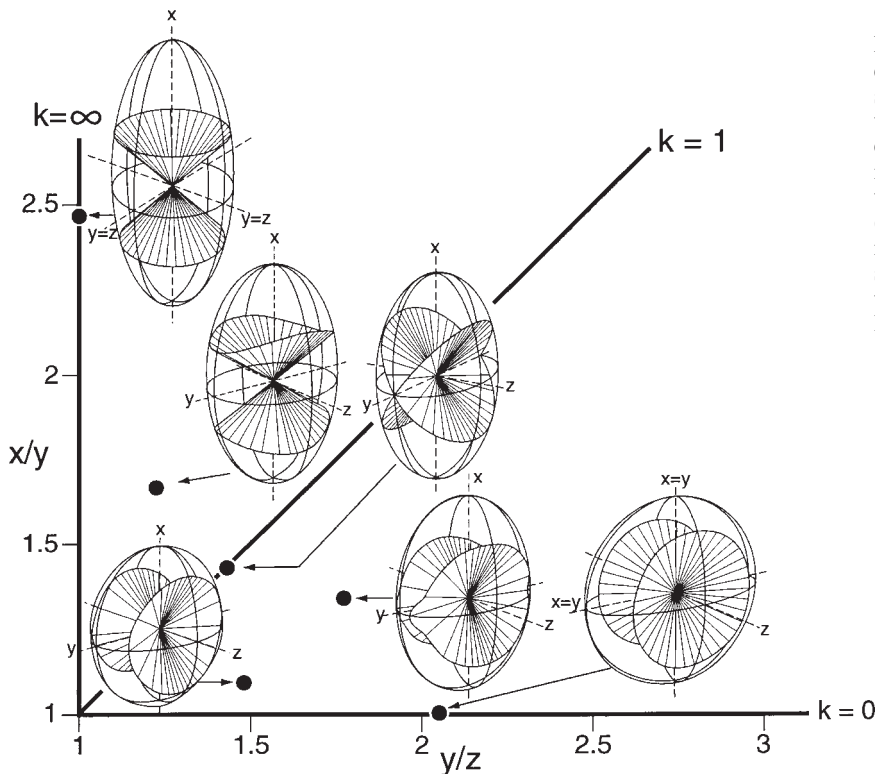


Fig. 9. Flinn diagram with examples of flattening, plane strain and constriction ellipsoids, the cones or planes inside the ellipsoids outline the surfaces of no finite longitudinal strain. The three lowermost ellipsoids are (left to right) from locality 2-north, locality 1 and locality 2-south (compare with Fig. 10 and the text). The ellipsoid at the $k=0$ line is from locality 3.

aplite and pegmatite veins cross-cut the contacts of the dykes and are folded with differently oriented axes or boudinaged within the dykes (Fig. 4b), whereas they are completely undeformed within the banded amphibolite. From the discussion above it is clear that the deformation is younger than dyke emplacement, while deformation of the early sheet veins and younger transsecting veins appear synchronous. Various oriented fold axes (see Fig. 12) are developed as a consequence of simultaneous deformation of differently oriented planar veins.

One of the dykes at this locality was chosen for a more detailed investigation (shown with an arrow on Fig. 8). At low water level in the lake it is situated along the shore but only one contact of the dyke is exposed. All the relationships described above are well-illustrated in this dyke (Figs 4b, 5b, 5c). The monzonite has a well defined lineation subparallel to the foldaxes in the old sheet veins and some of the younger veins and a foliation at an angle of approximately 30-40 degrees with the contact of the dyke.

Several pegmatite veins cross the dyke contact. On the host rock side, they form a large angle with the contact, while within the dyke, they have been rotated dextrally, thinned and boudinaged (Fig. 4b).

Strain analyses

At the three localities described above (Fig. 1), analyses were carried out to investigate, and if possible, to quantify strain inside the monzonite dykes.

As a starting point, it was assumed that:

- 1) no volume change has affected the monzonites during their deformation;
- 2) there has been no layer parallel shortening in the thin (1 mm to 2 cm) veins prior to or during their folding;
- 3) the bulk strains inside each dyke (or at least the part of the dyke where measurements were collected) was homogeneous, justifiable because of the uniform fold patterns in veins that cross-cut the dyke;
- 4) the sidewall rock is undeformed.

In constant volume strain ellipsoids, surfaces of no finite longitudinal strain (s.n.f.l.s.) separate the shortening sectors, where all directions are shortened, from the extensional sectors, where all directions are stretched. In the case of a plane strain the s.n.f.l.s. are two planes that intersect each other along the Y-axis of the strain ellipsoid. In all other cases the s.n.f.l.s. have the form of a double cone with opening angles $> 90^\circ$ and apical axis along the Z-axis for oblate flattening ellipsoids (Flinn's k value < 1 (Flinn 1962)), while opening angles are $< 90^\circ$ and the apical axis is along

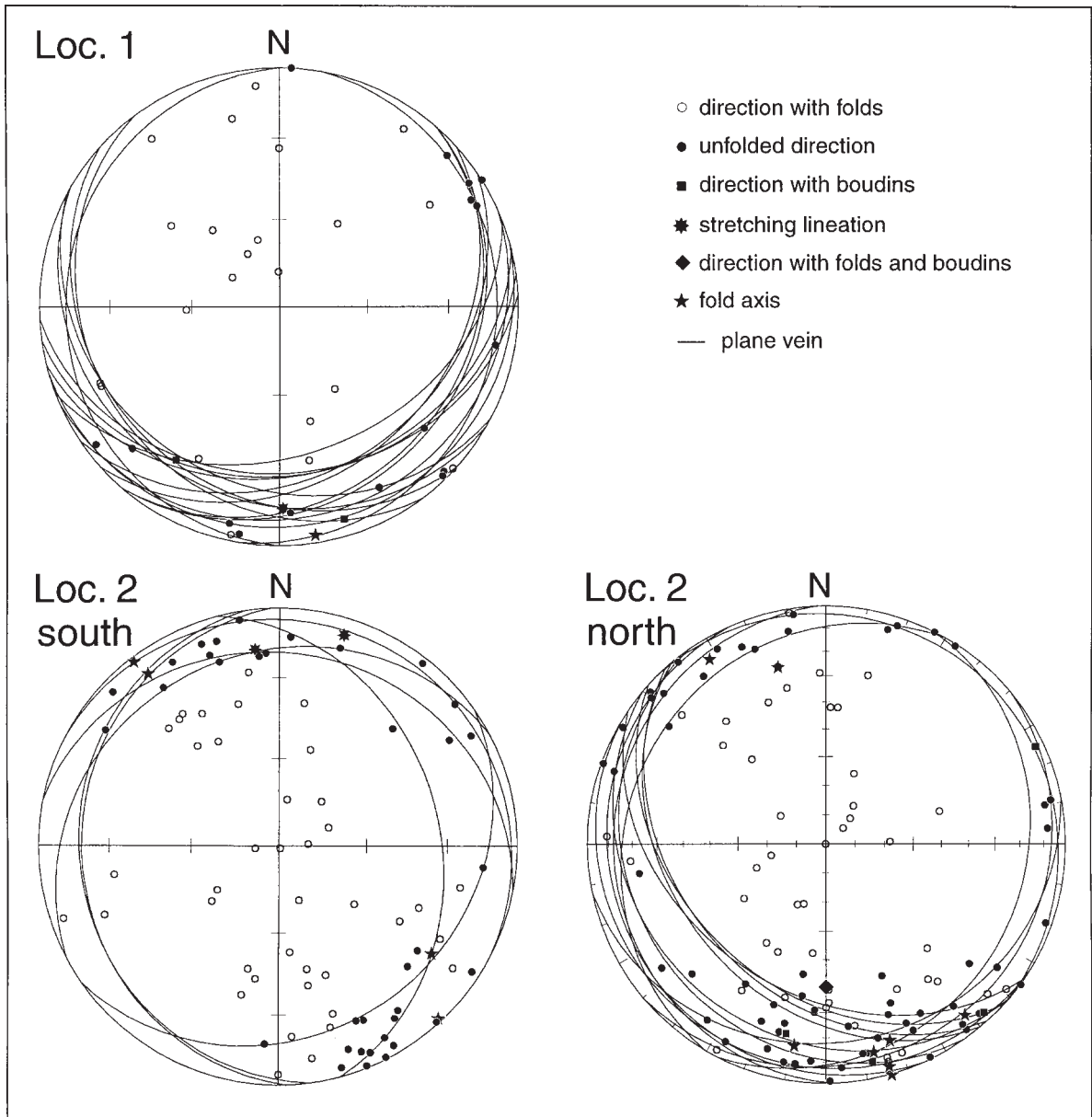


Fig. 10. Plots showing measured orientations of vein traces and unfolded veins (great circles) in the monzonite dykes at locality 1 and 2. Equal area projections, lower hemisphere.

the X-axis for prolate (constrictional) ellipsoids ($k > 1$). For a full discussion see Flinn (1962) and Ramsay & Huber (1983). Figure 9 shows a Flinn diagram with examples of strain ellipsoids and the shapes of their s.n.f.l.s.

The shape and opening angles of the s.n.f.l.s. determine the shape of the strain ellipsoid and thus the strain parameters, the mathematical solutions are given in the appendix. In order to establish the s.n.f.l.s. for the monzonites, directions of vein traces were measured at differently oriented outcrop surfaces at each local-

ity, and it was noted whether they were folded, straight or boudinaged. The orientations of the traces were plotted on stereonet projections together with measured strikes and dips of planar veins (Fig. 10).

This method is modified from the method used by Talbot (1970), who plotted poles to folded and planar or boudinaged veins. The modification is necessary because, at the studied localities, it was not possible to measure the strike and dip of folded veins as this requires that relatively large portions of the folded surfaces of the veins are exposed. The modification

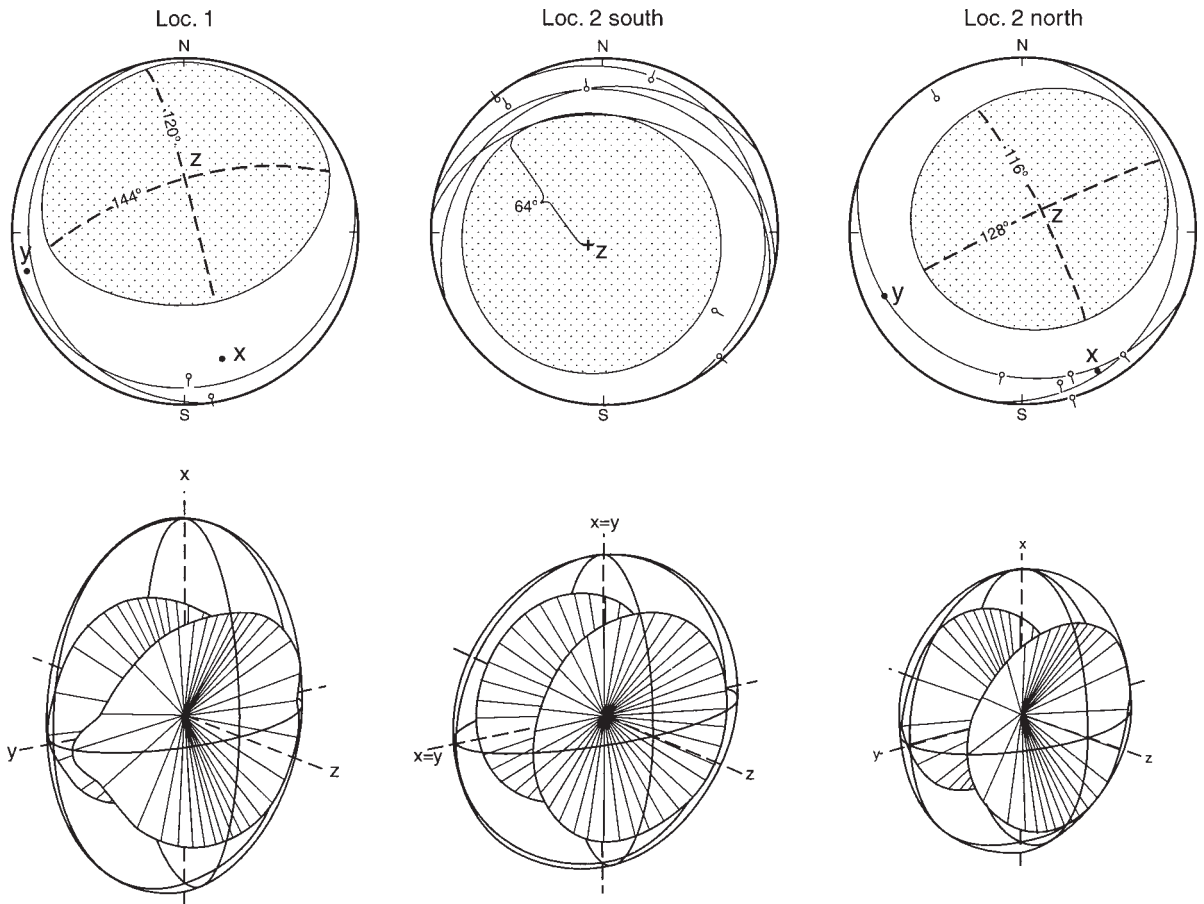


Fig. 11. Above: equal area projections showing shortening fields (stippled) and extension fields; great circles indicate measured foliations and o- indicates a measured fold axis. Below: shapes of the corresponding strain ellipsoids and their surfaces of no finite longitudinal strain, notice that the flattening planes (the XY planes) are vertical in these Figures, while they are subhorizontal at the localities as seen in the stereonet projections above.

has no implications for the theoretical background to the strain analysis.

In the study by Talbot (1970), poles to folded veins and poles to extended veins plot in the stereographic projection on each side of a surface that is complementary to the s.n.f.l.s. Provided that the deformation was homogeneous and enough measurements have been obtained, this surface is well defined.

In the present study, all vein traces that plot in the shortening field of the stereonet projections show folds whereas in the extensional field, the vein traces are either straight, boudinaged or folded. The reason why traces of folded veins are distributed throughout the stereographic projections (Fig. 10) is that the traces of a folded vein appear folded in all sections except in those parallel to the fold axis. If the folds are non-cylindrical, all sections show folds. Folded veins have elongations < 0 in some directions and ≥ 0 in others. Non-folded and boudinaged veins have elongations ≥ 0 in all directions and the great circles representing

non folded veins on the stereonet lie fully within the extension field. Only relatively thick pegmatitic veins (more than 1–2 cm) are boudinaged which may indicate that thinner veins can take up some extension by thinning instead of breaking or the distance between necking points may be very large. Talbot (1970) showed that for thin veins, low viscosity contrast between vein and host rock and low strain rate favor thinning without necking of extended veins. He also showed that veins that have been shortened in some directions and extended in others show folds while boudins are exceptional. He concluded that for necks to develop, the vein must be wholly extended (extended in all directions parallel with the vein). From the present study it appears that even wholly extended thin veins show no necking.

In the analyses presented here, the s.n.f.l.s. has been drawn as close as possible to the extended directions, i.e. with the largest opening angles that are in accordance with the data (compare Figs 10 and 11), this is to

Table 1. Calculated strain parameters from monzonite dykes at locality 1, 2 and 3. ψ_{xz} and ψ_{yz} are the angles between the X and Y axes respectively and the s.n.f.l.s., x, y and z are the lengths of the major, intermediate and minor strain axes ($= \lambda_1^{1/2}$, $\lambda_2^{1/2}$ and $\lambda_3^{1/2}$ see appendix); k is the Flinn value and γ is the shear value.

	Loc. 1	Loc. 2-south	Loc. 2-north	Loc. 3
Assumptions	No volume change, veins fold immediately when shortened, bulk homogeneous strain in dykes.			Simple shear deformation, no vol. change
Strain parameters	$\psi_{xz} = 30^\circ$ $\psi_{yz} = 18^\circ$ x = 1.47 y = 1.10 z = 0.62 k = 0.47 x/z = 2.37	$\psi_{xz} = 26^\circ$ $\psi_{yz} = 26^\circ$ x = 1.27 y = 1.27 z = 0.62 k = 0 x/z = 2.05	$\psi_{xz} = 32^\circ$ $\psi_{yz} = 26^\circ$ x = 1.21 y = 1.11 z = 0.75 k = 0.18 x/z = 1.61	$\psi_{xz} = 31^\circ$ $\gamma = 1.06$ x = 1.66 y = 1.00 z = 0.60 x/z = 1.77
Assumption	No volume change in veins			
Max. hom. vol. reduction in monzonite	9%	8%	3%	
Length of strain axes	x = 1.16 y = 1.04 z = 0.75	x = 1.10 y = 1.10 z = 0.76	x = 1.09 y = 1.05 z = 0.85	
Assumptions	Strain is simple shear + max. hom. vol. reduction in monzonite			
Max. prefolding shortening in veins	4%	9%	5%	

account for the pronounced shortening observed within steep dykes. The accuracy of the opening angles and the exact orientations of the strain axes depend on a complete sample of directions showing extension. More narrow opening angles imply lower strains (shorter X- and/or Y-axes and longer Z-axis) and the strain ellipsoids plot closer to the origin of the Flinn diagram. The flattening type of the strain ellipsoid and the overall directions of the strain axes remain the same, even if the opening angles are more narrow.

Localities 1 and 2

At locality 2, the northern (including the middle) and the southern parts of the dyke were analysed separately. The three stereo plots from localities 1 and 2 (Fig. 10) show that the s.n.f.l.s. form conical surfaces that are compatible with flattening strain ellipsoids with steep Z-axes (Fig. 11). At locality 1 and 2-north the interpolated strain ellipsoids are triaxial, with Y-axes plunging to the SW and X-axes plunging to the SE, while at locality 2-south, it is axial symmetric.

Mathematical equations for determining the strain parameters for flattening strain ellipsoids with known opening angles of the s.n.f.l.s. are given in the appendix, and the results of such strain calculations for the two localities are given in Table 1.

At the two localities the monzonite has intruded into a coarse grained granite (loc. 1) and a migmatitic orthogneiss (loc. 2). In the side-walls neither of these host rocks show visible signs of the deformation which has affected the monzonite dykes. As the veins are sometimes seen to cross-cut the margins of the dykes without being disrupted, although they change direction (Fig. 5e), there must exist strain compatibility across the margins (Ramsey & Huber 1983). Thus, the boundaries of the dykes should be planes of no finite strain, which is incompatible with a flattening strain inside the dykes, as no such planes exist in a flattening strain ellipsoid. Clearly something must be wrong with the assumptions, so it is necessary to re-consider these.

Discussions of assumptions. An invalidation of the first assumption, about constant volume in the monzonite, may afford a partial solution to the apparent flattening ellipsoid problem. But it can only be a partial solution, because in a flattening ellipsoid with no elongation along the λ -axis ($\lambda_2^{1/2} = 1$) all veins should be folded, except those that contain the Y-axis and have small angles with the X-axis. However, many veins that do not contain the Y-axis are not folded (Fig. 10).

The maximum possible volume reduction that is compatible with the detected position of the s.n.f.l.s. (Fig. 11) can be calculated from the equations (5)–(11) given in the appendix, and the derived values of

the strain axes and of the maximum volume reduction at the two localities are listed in Table 1.

A breakdown of the second assumption, that veins start to fold immediately when they are shortened without any initial layer parallel shortening, may also contribute to a solution of the conflict between an apparent flattening strain inside the dyke and the requirement of strain compatibility across the contacts.

Wavelength-thickness relationships have been measured in a number of veins at locality 2 in order to determine the viscosity contrast, μ_1/μ_2 , between the granitic veins and the monzonite matrix. The method of Ramsay & Huber (1987, p. 390) gave values of μ_1/μ_2 ranging from 7–30. With such relatively low viscosity contrasts, initial layer parallel shortening is possible. Hudleston & Stephansson (1973) showed that in buckling experiments and finite element models, some layer parallel shortening took place before significant folding was apparent except for extremely high viscosity contrasts. For low viscosity contrasts, layer parallel shortening continued during fold development (Hudleston 1973).

In the case of synfolding layer shortening, wavelength (measured along the central line in the layer) is shorter and layer thickness is greater than the initial dimensions, and the viscosity contrast is then underestimated.

If the veins have taken up some layer parallel shortening prior to their folding, then what appeared to be the s.n.f.l.s. is in reality not a surface defined by directions with unit lengths. Instead it is a surface containing the lines that have taken up the maximum of prefolding layer parallel shortening. The apparent s.n.f.l.s. is then a surface defined by all directions that have been shortened by a certain amount. This implies that the shape of the previously calculated strain ellipsoid is correct, but its axes are shorter than were calculated.

If the true deformation is a simple shear, with or without additional volume reduction, then $\lambda_2^{1/2} = 1$, because the Y-axis lies in the shear plane, which for compatibility reasons is unstrained. The real magnitude of elongation in any direction in the true strain ellipsoid is found by multiplying the previously calculated values by $\lambda_2^{-1/2}$. The true longitudinal strain of the lines in the apparent s.n.f.l.s. is 1 times $\lambda_2^{-1/2}$. The two planes that define the true s.n.f.l.s. contain the Y-axis and form angles ψ_{xz} with the X-axis that can be found from equation (5) in the appendix.

The calculated maximum prefolding layer parallel shortening of the veins for a simple shear deformation is given in Table 1. The value for locality 2-south is the double of the values for localities 1 and 2-north. At this locality the strain ellipsoid is rotationally symmetric with identical elongations along the X and Y axes. Consequently, a simple shear solution combined with volume reduction implies that no veins have been extended. They have either undergone layer parallel shortening, or both layer parallel shortening and fold-

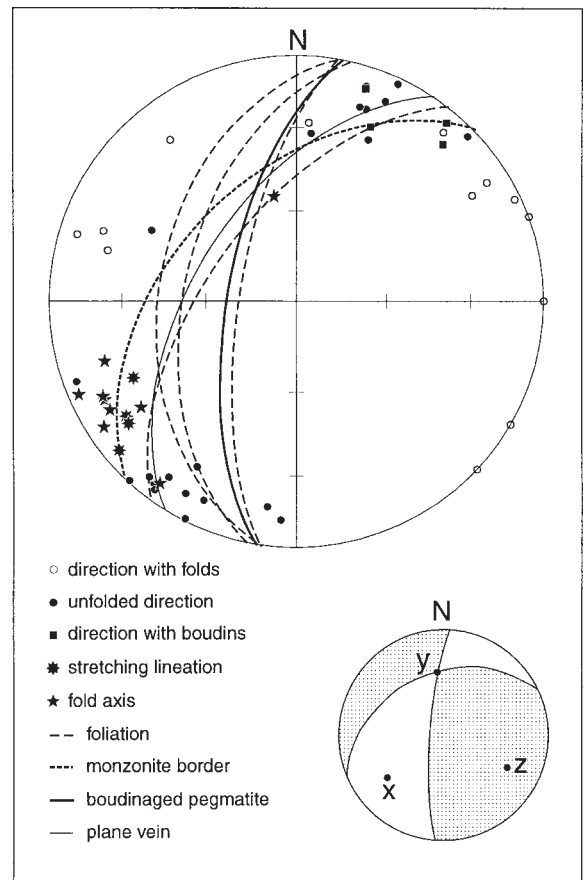


Fig. 12. Above: equal area projection of structural elements measured at locality 3. Below: shortening fields (stippled) and extension fields.

ing. Only veins parallel to the XY plane are unstrained.

Assumption three, concerning bulk homogeneous strain is perhaps the most difficult to assess. Clearly, irregular contacts should introduce some heterogeneity close to the contacts. However, in dykes with overall parallel contacts, as at locality 1, the strain may be largely homogeneous.

In highly irregular dykes, as the one at locality 2, it seems unrealistic for geometrical reasons to assume a homogeneous bulk strain throughout the entire volume of the dyke unless the host rock is simultaneously deformed. Assumption four may therefore fail to be fulfilled, at least at locality 2. Burg et al. (1986) showed that in experimentally deformed polycrystalline ice, a visible shape fabric was not formed at a shear strain of 10%, they also suggested that ice could be used as an analogue of easily deformed quartz-rich rocks. If, at locality 2, the host rock has actually been deformed contemporaneously with the deformation in the monzonite, the shortened veins in the host rock must have taken up the deformation by layer parallel shortening, as they are not folded.

Locality 3

Figure 12 shows a steronet plot of the orientational data collected at locality 3. Although the data are not absolutely consistent, an attempt has been made to delimit an extension field from a shortening field by two planes suggesting a plane strain ellipsoid with a shortening axis plunging moderately to the southeast (Fig. 12). Field relations indicate that the deformation at this locality is a simple shear with a shearing direction plunging at a low angle to the ESE.

From equations (12) and (13) in the appendix, the shear strain and the lengths of the strain axes have been calculated. The results are given in Table 1 and agree with the shape and orientation of elongate aggregates occurring in the monzonite at this locality.

In simple shear deformation, the shear plane should coincide with dyke contacts as this is a s.n.f.l.s., and in a bulk homogeneous deformation, the fabric elements should have uniform orientations. In the data samples shown in Figure 12, this is not quite the case, which may be explained by the difficulty of obtaining accurate measurements of the foliation and the dyke contact. Also, foliation deviates close to folded veins and the dyke contact changes orientation slightly along its strike (Fig. 8).

Discussion of strain determinations and observations

From the considerations described above, it may be theoretically possible to describe the strain inside the monzonite dykes as a homogeneous simple shear, with, in some cases, an additional volume reduction in the monzonite and prefolding layer parallel shortening in the granitic veins.

A simple shear deformation in the monzonite dykes, induced by a relative displacement of the two sidewall blocks, affords the best solution to the deformation in planar dykes. In many narrow dykes, this solution seems obvious (Figs 4a, 4f). At locality 1, the solution implies a relative movement of the overlying block in a subhorizontal NNW direction (Fig. 11) away from the center of the Høvringsvatn complex. At locality 3, the strain in the dyke has developed during a displacement of the upper northwestern host rock block towards the ENE in a combined dextral and upwards movement (Fig. 12) almost tangentially to the Høvringsvatn ring complex.

The dyke at locality 2 has a much more irregular geometry (Fig. 7) than the dykes at the other two localities which is in itself preventive to the development of homogeneous strain throughout the dyke. Also, from geometrical considerations, a simple shear deformation in the dyke is not possible unless parts of the host rock are also deformed. Alternative models for the deformation pattern at locality 2 are constrained by requirements for continuity and strain compatibil-

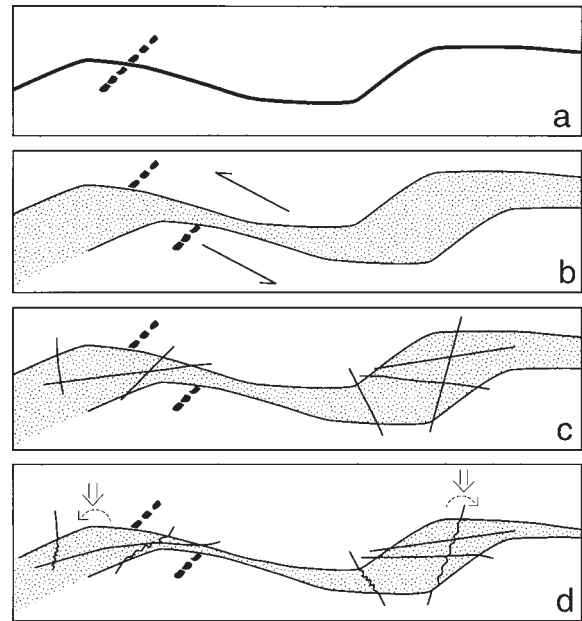


Fig. 13. Simplified cartoon to illustrate the formation of the monzonite dyke at locality 2 (a to b), the emplacement of the granitic veins (c) and a model for the deformation and development of the internal structures (d). The horizontal length of the section is approx. 35 m.

ity across the dyke contacts. One possibility is sketched in Figure 13. According to this model, the emplacement of the dyke took place during a combined shear and tensional opening of a stepped fracture. At a later stage, the dyke was criss-crossed by the granitic veins. The deformation in the dyke reflects an overall vertical collapse with a vertical shortening across the dyke, volume reduction in the dyke, and oppositely directed rotations of the two parts of the block overlying the dyke.

In these analyses, it was assumed that during deformation inside the monzonite dykes, no penetrative strain was accommodated by the host rocks, regardless of their age or composition. This assumption seemed justified by the apparent lack of (syndeformational) fabric development and the existence of planar, seemingly undeformed, granitic veins in the host rocks. However, this aspect deserves further consideration.

In many minor monzonitic bodies of limited lateral extent, the internal deformation structures are, for geometrical reasons, extremely difficult to explain unless a concomitant more-or-less penetrative strain has been taken up by the host. Talbot (1982) and Talbot & Sokoutis (1992) claimed that the lack of fabric in the host rock adjacent to highly deformed dykes is merely a matter of the former being less fabric-responsive to strain. They interpreted the cusped structures at dyke margins to result from a common deformation. In the examples they describe, no cross-cut-

ting veins are described to occur, which makes their interpretation more probable than for the Setesdalen area.

The development of deformation structures such as folds and boudins in single layers or veins depends on the existence of a viscosity contrast between vein and matrix, the first being most competent. If, during deformation, granitic veins and host rocks have similar viscosities, while the monzonite dykes are much more incompetent, a situation with apparently undeformed veins in the host rock could arise. The strain in the host rocks, and in the veins in them, may have been taken up by a recrystallization-accommodated grain boundary sliding, which would not result in a fabric development. A main objection to the general acceptance of this hypothesis is the unlikelyhood that the various host rocks had similar viscosities during deformation. The acid host rocks, whose compositions and viscosities lie close to the granitic veins, are the most probable candidates for having taken up some strain. A detailed microstructural investigation of the various rock types might help to solve these questions, but is outside the frames of this study.

In the light of the discussion above, the flattening strain ellipsoid at locality 1 may result from a plane strain simple shear in the dyke combined with a small flattening in both dyke and host rock. The flattening component led to 4% stretching along the Y-axis (Table 1) and no volumetric reduction in the monzonite is necessary.

At locality 2, the situation is more complex because of the irregular geometry of the dyke. Cuspate structures are abundant, especially on the steeper parts of the margins of the dyke (Figs 4h, 7). A hidden deformation of the granitic gneiss host rock cannot be ruled out. The model shown in Figure 13 implies some deformation, or at least adjustments, perhaps along fractures in the upper host rock block.

At locality 3, the strain in the dyke was interpreted as a simple shear between rigid, unstrained, amphibolite host rock blocks.

Conclusions

The late kinematic monzonite dykes and other minor intrusions in the Setesdalen area were generated by the stress systems in and around a number of central magmatic complexes during and immediately following the emplacement of these. They were emplaced into a semibrittle, warm environment.

While many of the dykes appear to have intruded under simple tensional local conditions, the intrusion of others were accompanied by a tangential shear displacement along the fracture.

Shear movements along stepped fractures led to the formation of transtensional openings that were filled with the monzonite magma.

The formation of crosscutting veins constitutes a

chronological separation between the intrusion of the dykes and the development of their internal deformation structures.

The present fabric pattern in the dykes mainly reflects a deformation following granitic vein emplacement which caused folding or stretching of the veins inside the dykes.

The deformation structures in the dykes fully or mainly reflect a simple shear deformation. An apparent minor component of flattening strain, as seen from some of the strain analyses, is explained by either volume reduction of the monzonite and pre-folding layer parallel shortening of the granitic veins or by a contemporaneous component of flattening in both dyke and sidewall rock.

For irregular dykes, some localized deformation in the sidewall rock seems unavoidable for geometrical reasons.

The type and amount of strain within the dykes, the orientation of the strain axes, and the sense and direction of displacement of the side wall blocks vary from one dyke to the other.

The deformation structures in the dykes are considered to be a consequence of the late phases of differential collapse and cauldron subsidence following the emplacement of the central intrusive complexes in the Setedal area. The strain was preferentially accumulated in the incompetent monzonite dykes and minor bodies while the more rigid host rock blocks were mainly passively displaced in various directions.

Acknowledgements

Valuable comments and suggestions to the manuscript were made by Niels Østerby Olesen and two anonymous referees. Thanks are due to Dr. Susan Stipp who kindly improved the English text and to René Madsen who drafted the figures.

Dansk sammendrag

I Setesdalen området i det centrale Syd Norge optræder et meget stort antal, ofte uregelmæssige, monzonitiske gange og mindre legemer. De blev intruderet i varme omgivelser under de seneste stadier af den Sveconorwegiske magmatiske aktivitet i området (for ca. 900 millioner år siden). Nogle af gangene danner systemer af keglegange og klokkegange (bell-jar sheets) som hører til nogle magmatiske ringkomplekser i området. Gangenes uregelmæssige form skyldes tildels, at sidestenen var varm og derfor forholdsvis blød ved deres intrusion, dels at gangene udfylder hulrum der er opstået ved åbning af uregelmæssige sprækker.

Monzonitgangene udmærker sig ved at vise tegn på,

at de har været udsat for en kraftig intern deformation, som ikke har sat sig synlige spor i de øvrige bjergarter. Monzoniterne er folierede og linierede og gennemsættende granitårer er blevet ptygmatiske foldet eller er blevet strakt, undertiden boudineret. De samme granitiske årer viser ikke tegn på deformation når de gennem sætter sidestenen til monzonitgangene, uanset om sidestenen er en magmatisk bjergart tilhørende et ringkompleks, eller er en ældre gnejs eller amfibolit. Dannelsen af de granitiske årer betegner en tidsadskillelse mellem intrusionen af gangene og deformationen af dem.

Strainanalyser tyder på, at deformationen i monzonitgangene i hovedsagen er fremkommet ved, at stive sidestensblokke har forskudt sig i forhold til hinanden, hvorved de mere bløde gangbjergarter er blevet plastisk deformerede. I nogle tilfælde synes det uundgåeligt, bl.a. af geometriske årsager, at der må være sket en mindre samtidig deformation også i sidestenen, selv om denne ser udeformeret ud.

References

- Allart, J.H. 1967: Basic and intermediate igneous activity and its evolution of the Julianehåb Granite, South Greenland. *Meddelelser om Grønland* 175, 136 pp.
- Andersen, T., Hagelia, P. & Whitehouse, M.J. 1994: Precambrian multi-stage crustal evolution in the Bamble sector of south Norway: Pb isotopic evidence from a Sveconorwegian deep-seated granitic intrusion. *Chemical Geology* 116, 327–343.
- Anderson, E.M. 1936: The dynamics of the formation of cone-sheets, ring-dykes and cauldron subsidence. *Proceedings of the Royal Society of Edinburgh* 56, 128–157.
- Baer, G. & Blyth, M. 1990: A mechanism of dyke segmentation in fractured host rock. In Parker, A.J., Rickwood, P.C. & Tucker, D.H. (eds) *Mafic dykes and emplacement mechanisms*, 3–11. Balkema, Rotterdam.
- Berger, A.R. 1971: Dynamic analysis using dikes with oblique internal foliations. *Geological Society of America Bulletin* 82, 781–786.
- Berthelsen, A. 1980: Towards a palinspastic tectonic analysis of the Baltic shield. (Colloque C6: Géologie de l'Europe du Précambrien aux Bassins sédimentaires post-hercyniens.) *Congres Géologique International*, Paris 108, 5–21.
- Berthelsen, A. 1987: A tectonic model for the crustal evolution of the Baltic Shield. In Schaer, J.P. & Rodger, J. (eds) *The anatomy of mountain ranges*, 31–58. Princeton University Press, Princeton, N.J.
- Bingen, B., Demaiffe, D. & Van Bremen, O. 1996: Rb-Sr isotopic signature of augen gneiss suites in the Sveconorwegian province of SW Norway. In Demaiffe, D. (ed.) *Petrology and geochemistry of magmatic suites of rocks in the continental and oceanic crusts*. A volume dedicated to professor Jean Michot, 161–174. Université Libre de Bruxelles. Royal Museum for Central Africa (Tervuren).
- Bjørlykke, H. 1934: The mineral paragenesis and classification of the granite pegmatites of Iveland, Setesdal, southern Norway. *Norsk Geologisk Tidsskrift* 14, 211–311.
- Bjørlykke, H. 1937: The granite pegmatites of southern Norway. *The American Mineralogist* 22, 241–255.
- Burg, J.P., Wilson, C.J.L. & Mitchell, J.C. 1986: Dynamic recrystallization and fabric development during the simple shear deformation of ice. *Journal of Structural Geology* 8, 857–870.
- Davidson, L.M. & Park, R.G. 1978: Late Nagssugtoqidian stress orientation derived from deformed granodiorite dykes north of Holstensborg, West Greenland. *Journal of the Geological Society of London* 135, 283–289.
- Falkum, T. & Pedersen, S. 1979: Rb-Sr age determinations on the intrusive Precambrian Homme granite and consequences for dating the last regional folding and metamorphism in the Flekkefjord region, SW Norway. *Norsk Geologisk Tidsskrift* 59, 59–65.
- Falkum, T. & Petersen, S. 1980: The Sveconorwegian Orogenic Belt, a case of Late-Proterozoic plate-collision. *Geologischen Rundschau* 69, 622–647.
- Flinn, D. 1962: On folding during three dimensional progressive deformation. *Quarterly Journal of the Geological Society of London* 118, 385–433.
- Hansen, K., Pedersen, S., Fought, H. & Stockmarr, P. 1996: Post-Sveconorwegian exhumation and cooling history of the Evje area, southern Setesdal, Central South Norway. *Geological Survey of Norway Bulletin* 431, 49–58.
- Hudleston, P.J. 1973: An analysis of “single-layer” folds developed experimentally in viscous media. *Tectonophysics* 16, 189–214.
- Hudleston, P.J. & Stephansson, O. 1973: Layer shortening and fold-shape development in the buckling of single layers. *Tectonophysics* 17, 299–321.
- Johnson, M.R.W. & Dalziel, I.W.D. 1966: Metamorphosed lamprophyres and the late thermal history of the Moines. *Geological Magazine* 103, 240–249.
- Kaitaro, S. 1953: Geologic structure of the late Precambrian intrusives of the Åva area, Åland Islands. *Bulletin de la Commission Géologique de Finlande* 162, 71 pp.
- Kuenen, Ph.H. 1967: Origin of ptygmatic features. *Tectonophysics* 6, 143–158.
- Miller, W.J. 1945: Observations on pseudodikes and foliated dikes. *Journal of Geology* 53, 175–190.
- Park, R.G., Åhäll, K.I. & Boland, M.P. 1991: The Sveconorwegian shear-zone network of SW Sweden in relation to mid-Proterozoic ålate movements. *Precambrian Research* 49, 245–260.
- Pedersen, S. 1975: Intrusive rocks of the northern Iveland-Evje area, Aust-Agder. *Norges Geologiske Undersøkelse* 322, 1–11.
- Pedersen, S. 1981: Rb-Sr age determinations of Late Proterozoic granitoids from the Evje area, south Norway. *Bulletin of the Geological Society of Denmark* 29, 129–143.
- Pedersen, S. & Konnerup-Madsen, J. 2000: Geology of the Setesdal area, South Norway: Implications for the Sveconorwegian evolution of South Norway. *Bulletin of the Geological Society of Denmark* 46 (this volume).
- Ramberg, H. 1960: Relationship between length of arc and thickness of ptygmatically folded veins. *American Journal of Science* 258, 36–46.
- Ramsay, J.G. 1967: *Folding and fracturing of rocks*, 568 pp. McGraw-Hill, New York and London.

- Ramsay, J.G. & Huber, M.I. 1983: The techniques of modern structural geology volume 1: strain analysis, 307 pp. Academic Press, London.
- Ramsay, J.G. & Huber, M.I. 1987: The techniques of modern structural geology volume 2: folds and fractures, 308–700. Academic Press, London.
- Roberts, J.L. 1970: The intrusion of magma into brittle rocks. In Newall, G. & Rast, N. (eds) Mechanism of igneous intrusion. Geological Journal Special Issue 2, 287–338. Seel House Press, Liverpool.
- Ryan, B. 1995: Morphological features of multigeneration basic dykes near Nain, Labrador: clues to origin emplacement mechanisms and subsequent deformation. *Precambrian Research* 75, 91–118.
- Skjerna, L. 1975: Experiments on superimposed buckle folding. *Tectonophysics* 27, 255–270.
- Skjerna, L. & Pedersen, S. 1982: The effects of penetrative Sveconorwegian deformations on Rb-Sr isotope systems in the Rømskog – Aurskog-Höland area, SE Norway.
- Starmer, I.C. 1993: The Sveconorwegian Orogeny in southern Norway, relative to deep crustal structures and events in the North Atlantic Proterozoic Supercontinent. *Norsk Geologisk Tidsskrift* 73, 109–132.
- Talbot, C.J. 1970: The minimum strain ellipsoid using deformed quartz veins. *Tectonophysics* 9, 47–76.
- Talbot, C.J. 1982: Obliquely foliated dikes as deformed incompetent single layers. *Geological Society of American Bulletin* 93, 450–460.
- Talbot, C.J. & Sokoutis, D. 1992: The importance of incompetence. *Geology* 20, 951–953.
- Watterson, J.S. 1968: Plutonic development of the Ilordleg area, South Greenland, Part II: Late kinematic basic dikes. *Meddelelser om Grønland* 185, 104 pp.
- Wiebe, R.A. & Collins, W.J. 1998: Depositional features and stratigraphic sections in granitic plutons: implications for the emplacement and crystallization of granitic magma. *Journal of Structural Geology* 20, 1273–1289.

Appendix

Determination of strain in flattening strain ellipsoids
From the angles ψ_{xz} and ψ_{yz} , which are the angles between the X and Y axes and the s.n.f.l.s. in the XZ and YZ planes respectively, it is possible to calculate the axial ratios of an oblate strain ellipsoid from the following equations (see Talbot 1970):

$$\cos^2 \psi_{xz} = m = \frac{a^{-2/3} b^{2/3} - b^2}{a^2 - b^2} \quad (1)$$

$$\cos^2 \psi_{yz} = n = \frac{a^{-2/3} b^{2/3} - b^2}{1 - b^2} \quad (2)$$

where

$$a = \left(\frac{\lambda_1}{\lambda_2} \right)^{1/2} \quad \text{and} \quad b = \left(\frac{\lambda_2}{\lambda_3} \right)^{1/2}$$

λ_1 , λ_2 and λ_3 are the quadratic extensions.
Combining (1) and (2) gives:

$$b^2 = \frac{-A \pm \left[A^2 + 4 \left(\frac{n}{1-n} \right)^3 \right]^{1/2}}{2}$$

$$\text{and} \quad \frac{1}{a} = \frac{[b^2(1-n) + n]^{3/2}}{b}$$

$$\text{where} \quad A = \frac{(1-n)^2(1+2n) + \left(\frac{n}{m} - 1 \right)}{(1-n)^3}$$

If there is no volume reduction: $(\lambda_1 \lambda_2 \lambda_3)^{1/2} = 1$ (3)

and the length of each of the axes of the strain ellipse can be found from:

$$y^2 = \lambda_2 = \left(\frac{b^2}{a^2} \right)^{1/3}$$

$$x^2 = \lambda_1 = a^2 \lambda_2$$

$$z^2 = \lambda_3 = \frac{\lambda_2}{b^2}$$

The k value is calculated from

$$k = \frac{a-1}{b-1} \quad (4)$$

Determination of maximum volume reduction

The maximum possible volume reduction that is compatible with the detected position of the s.n.f.l.s. (Fig. 10) can be calculated:

$$\tan^2 \psi_{xz} = \frac{\lambda_3(\lambda_1 - 1)}{\lambda_1(1 - \lambda_3)} = \frac{1 - \frac{1}{\lambda_1}}{\frac{1}{\lambda_3} - 1} \quad (5)$$

$$\tan^2 \psi_{yz} = \frac{\lambda_3 (\lambda_2 - 1)}{\lambda_2 (1 - \lambda_3)}$$

and

$$V = (\lambda_1 \lambda_2 \lambda_3)^{1/2} = 1 + \Delta_v \quad (6)$$

(Ramsey & Huber 1983) where V is the volume of the strain ellipsoid and Δ_v is the volumetric dilatation.

If

$$\tan^2 \psi_{xz} = K_1, \quad \tan^2 \psi_{yz} = K_2$$

and

$$x_1, x_2 \text{ and } x_3 = \frac{1}{\lambda_1}, \frac{1}{\lambda_2} \text{ and } \frac{1}{\lambda_3}$$

by combining with (5) and (6) and reorganizing we get:

$$x_1 = 1 - K_1 x_3 + K_1 \quad (7)$$

$$x_2 = 1 - K_2 x_3 + K_2 \quad (8)$$

$$-x_2 x_1 = (V^2 x_3)^{-1} \quad (9)$$

multiplying (7) and (8) and inserting the result in (9) we arrive at the function:

$$f(x_3) = K_1 K_2 x_3^3 - (K_1 + K_2 + 2K_1 K_2) x_3^2 + (1 + K_1 + K_2 + K_1 K_2) x_3 - \frac{1}{V^2} = 0 \quad (10)$$

Differentiating equation (10) gives:

$$f'(x_3) = 3K_1 K_2 x_3^2 - 2(K_1 + K_2 + 2K_1 K_2) x_3 + (1 + K_1 + K_2 + K_1 K_2) = 0 \quad (11)$$

Solving equation (11) for x_3 give two roots, but only one of these gives a real value for V. Inserting x_3 in (7), (8) and (9) give the values of x_1 , x_2 and V, where V is the minimum volume that satisfies the measured shape of the s.n.f.s.

Determination of strain in plane strain ellipsoids

From the angle ψ_{xz} , it is possible to find the shear γ and the lengths of the strain axes in a plane strain ellipsoid from (Ramsay & Huber 1983, p. 30):

$$\tan 2\psi_{xz} = \frac{2}{\gamma} \quad (12)$$

and

$$x^2 \text{ or } z^2 = \lambda_1 \text{ or } \lambda_3 = \frac{1}{2}(\gamma^2 + 2 \pm \gamma(\gamma^2 + 4)^{1/2}) \quad (13)$$